# Solitary surface acoustic waves

C. Eckl,* A. S. Kovalev,† and A. P. Mayer
*Institute for Theoretical Physics, University of Regensburg, D-93040 Regensburg, Germany*

A. M. Lomonosov‡ and P. Hess
*Institute of Physical Chemistry, University of Heidelberg, D-69120 Heidelberg, Germany*
(Received 21 December 2003; published 11 October 2004)

Solitary acoustic pulses can propagate along the surface of a coated homogeneous and inhomogeneous medium. It is shown how these nonlinear surface acoustic waves evolve out of initial pulselike conditions generated by pulsed laser excitation and how they can be monitored by optical detection. The solitary pulse shapes at the surface are computed on the basis of an evolution equation with nonlocal nonlinearity. They depend on the anisotropy of the substrate. Various approaches for the derivation of the evolution equation from nonlinear elasticity theory are critically compared. The behavior of the solitary pulses in collisions is investigated and is found to strongly depend on the linear dispersion law. The nontrivial depth dependence of these solitary pulses is also analyzed.

DOI: 10.1103/PhysRevE.70.046604 PACS number(s): 43.25.+y, 68.35.Ja, 43.35.+d, 68.35.Gy

## I. INTRODUCTION

Solitary waves are pulselike entities of nonlinear excitations that propagate through a system without change of their shape [1]. The phenomenon of solitary waves is a ubiquitous one that has been observed and thoroughly studied in many branches of science, such as fluid dynamics, optics, plasma physics, etc. [2]. In the field of acoustic wave propagation in solids, comparatively few experimental studies have been reported with the aim of observing solitary waves. This is partly due to the difficulties encountered in exciting acoustic waves with sufficiently high intensity in a controlled way. Another important obstacle is the fact that the elastic nonlinearity in a solid is very small. As a rule, the higher-order elastic moduli of a solid are usually of the same order of magnitude as the second-order ones. Consequently, the ratio of nonlinear to linear terms in the governing equations for the displacements in the solids is given by a typical strain or acoustic Mach number, which can normally not exceed values of the order of 0.01, without causing fracture of the material.

The localization of solitary waves is achieved by an interplay of nonlinearity and dispersion. Since the equations of elasticity theory for a homogeneous elastic medium do not contain a length scale, dispersion of linear acoustic waves can occur only through length scales defined by the propagation geometry or due to coupling of the strains to other degrees of freedom. Here, we are not considering envelope-type solitons but the type of solitary waves that are formed when weak nonlinearity is matched by weak dispersion, similar to the classical solitons propagating in shallow water.

In the past, observations of strain solitary waves have been made in elastic rods using laser excitation [3]. In this case the dispersion of the relevant linear modes is due to the finite diameter of the rod. Very recently bulk acoustic solitary waves have been generated and observed [4]. Here, it was the discreteness of the underlying crystalline structure of the medium that gave rise to the dispersion of acoustic bulk waves of sufficiently high frequencies. A third type of solitary acoustic waves that has been realized experimentally by pulsed laser excitation are surface acoustic solitary pulses. Here, the dispersion is generated by covering the homogeneous elastic medium with a thin film made out of a suitable material to realize normal or anomalous dispersion [5,6].

Surface acoustic solitary pulses can be distinguished from the other two types of acoustic solitary waves in solids, realized up to now experimentally, by their two-dimensional character. The spatial extension of a solitary pulse in a rod along its axis is much larger than the diameter of the rod. As long as diffraction effects can be neglected, the strain fields associated with bulk acoustic solitons may be regarded as varying only along the direction of propagation. In comparison to these one-dimensional solitary waves, Rayleigh wave pulses or, more generally, surface acoustic wave (SAW) pulses have a nontrivial depth structure that extends into the elastic medium on the same length scale as the width of the pulse along the surface. In that respect, they are comparable to the lump soliton solution of the Kadomtsev-Petviashvili equation [7]. One goal of this paper is to analyze the depth dependence of surface acoustic solitary waves. Nevertheless, their associated strain distribution at the surface can be derived from a one-dimensional scalar evolution equation, from which the depth dependence of the displacement field is eliminated. However, this elimination leads to a nonlocal nonlinearity [8–11]. In the following section a derivation of this evolution equation is given, and it is shown explicitly that the approaches by Lardner [12], Parker [13–15] and the Hamiltonian approach used by Zabolotskaya, Hamilton, and

*Present address: Infineon Technologies AG, Balanstr. 73, D-81541 Munich, Germany.

†Permanent address: B. Verkin Institute for Low Temperature Physics and Engineering, Ukrainean Academy of Sciences, 310164 Kharkov, Ukraine.

‡Permanent address: General Physics Institute, 117942 Moscow, Russia.

 

co-workers [16–18] lead to the same result. We then present stationary pulse-type solutions of this evolution equation for different dispersion laws. Section IV contains a description of the experimental techniques used to launch surface acoustic pulses with finite amplitudes and to analyze their shapes at the surface. Experimental results are presented for the formation of a solitary pulse and compared with results of numerical simulations. In Sec. V, a numerical study of collisions of SAWs pulses is presented. It is found that such collisions are usually not elastic and that the collision scenario strongly depends on the dispersion law of linear SAWs. In particular, pulse collisions are found to be almost elastic if the linear dispersion term in the evolution equation is that of the Korteweg–de Vries (KdV) equation. A strong dependence on the type of linear dispersion is also demonstrated for the pulse evolution with initial conditions that are close to the shape of a solitary pulse (Sec. VI). Section VII is devoted to the construction of the depth profile of a solitary pulse and stationary periodic nonlinear surface waves, from the strain distribution at the surface. Numerical results for the depth profiles in different propagation geometries are given. The paper ends with a short conclusion.

## II. EVOLUTION EQUATION

A semi-infinite elastic medium is considered that fills the half-space $z<0$ in its undeformed state. It may be covered by a film filling the spatial region $0<z<d$. The elastic properties of this system are characterized by second-order elastic moduli $C_{\alpha\beta\,\mu\nu}$ and third-order elastic moduli $C_{\alpha\beta\,\mu\nu\,\zeta\xi}$. Moduli of higher order will not be taken into account in the following derivations. For the Cartesian indices we use small Greek characters. In order to keep the notation simple, we shall not introduce different sets of indices for the material and spatial coordinate systems. For the following, it is convenient to define the coefficients $S_{\alpha\beta\,\mu\nu\,\zeta\xi}=C_{\alpha\beta\,\mu\nu\,\zeta\xi}+\delta_{\alpha\mu}C_{\zeta\xi\,\beta\nu}+\delta_{\alpha\zeta}C_{\beta\xi\,\mu\nu}+\delta_{\mu\zeta}C_{\alpha\beta\,\nu\xi}$ [19]. The mass density $\rho$ and the elastic moduli of the system have to be regarded as being $z$ dependent.

The Lagrangian of the system is given by

$$\mathcal{L}=\int d^3x(E_k-E_p), \tag{2.1}$$

with the densities of the kinetic energy

$$E_k=\frac{1}{2}\rho\dot{u}_\alpha\dot{u}_\alpha \tag{2.2}$$

and potential energy

$$E_p=\frac{1}{2}C_{\alpha\beta\,\mu\nu}u_{\alpha,\beta}u_{\mu,\nu}+\frac{1}{6}S_{\alpha\beta\,\mu\nu\,\zeta\xi}u_{\alpha,\beta}u_{\mu,\nu}u_{\zeta,\xi} \tag{2.3}$$

up to terms of third order in the displacement gradients $u_{\alpha,\beta}=\partial u_\alpha/\partial x_\beta$. In Eqs. (2.2) and (2.3) and likewise in the remainder of this paper, a summation convention is invoked that implies summation over repeated Cartesian indices. One (two) dot(s) on top of a symbol stands (stand) for the first (second) derivative with respect to time. In Eq. (2.1), the volume integral refers to the material coordinates $x_\alpha$, $\alpha=1,2,3$, and we regard the displacement field as function of these material coordinates. In order to reduce the number of indices in the following equations, we shall use the symbols $x,y,z$ for $x_1,x_2,x_3$.

Applying Hamilton's principle, the equation of motion

$$\rho\ddot{u}_\alpha=\frac{\partial}{\partial x_\beta}T_{\alpha\beta} \tag{2.4}$$

for the displacement field follows, as well as the boundary conditions requiring that the Piola-Kirchhoff stress tensor components $T_{\alpha3}$ have to be continuous at the interface and zero at the free surface of the system. ($T_{\alpha\beta}=\partial E_p/\partial u_{\alpha,\beta}$.) In addition, we have to require the continuity of the displacement field at the interface, and for the description of waves excited at or near the surface, we have to impose the following conditions at $z\to-\infty$: The displacement field has either to vanish or the acoustic Poynting vector has to be directed into the medium; i.e., its $z$ component has to be negative. In the following, we consider the propagation of plane waves along the $x$ direction, and therefore let the displacement field be independent of the coordinate $y$.

Among the various ways of introducing dispersion for linear surface acoustic waves, we here consider theoretically two possibilities: (i) a film on the surface having acoustic properties different from those of the substrate and (ii) spatial variations of the mass density and/or elastic moduli of the substrate along the direction normal to the surface (graded material).

In case (i), the thickness $d$ of the film is chosen to be much smaller than typical wavelengths $\lambda=2\pi/q$ of the SAWs since the dispersion has to be sufficiently small. In this regime, one may eliminate the displacement field in the film in an expansion in powers of $qd$ to obtain an effective boundary condition [20,21], which has the form

$$\begin{aligned}T_{\alpha3}(x,0_-,t)=&-d\{\rho_F\ddot{u}_\alpha(x,0_-,t)-g^{(1)}_{\alpha\beta}u_{\beta,11}(x,0_-,t)\\&-g^{(2)}_{\alpha\beta\gamma}u_{\beta,11}(x,0_-,t)u_{\gamma,1}(x,0_-,t)\}\\&+d^2\{g^{(3)}_{\alpha\beta}\rho_F\ddot{u}_{\beta,1}(x,0_-,t)+g^{(4)}_{\alpha\beta}u_{\beta,111}(x,0_-,t)\}\\&+O(u^2d^2,u^3d,ud^3).\end{aligned} \tag{2.5}$$

Here, $\rho_F$ is the mass density of the film material. The coefficients $g^{(1)}_{\alpha\beta}$, $g^{(3)}_{\alpha\beta}$, and $g^{(4)}_{\alpha\beta}$ depend on the second-order elastic moduli of the film material, while $g^{(2)}_{\alpha\beta\gamma}$ depends on its second-order and third-order elastic moduli. Explicit expressions are given in Ref. [22]. The notation $0_-$ indicates that the corresponding quantity has to be taken on the substrate side at the interface between substrate and film.

In case (ii), we decompose the mass density and elastic moduli into an average value and a part varying with $z$:

$$\rho(z)=\overline{\rho}+\Delta\rho(z), \tag{2.6a}$$

$$C_{\alpha\beta\,\mu\nu}(z)=\overline{C}_{\alpha\beta\,\mu\nu}+\Delta C_{\alpha\beta\,\mu\nu}(z). \tag{2.6b}$$

In equations that contain the average quantities $\overline{C}_{\alpha\beta\,\mu\nu}$ and $\overline{\rho}$ only, we shall drop the overbars in order to simplify the notation. In equations where $C_{\alpha\beta\,\mu\nu}$ and $\rho$ stand for $z$-dependent quantities, their $z$ dependence is indicated ex-

plicitly to distinguish them from their average values.

We note here that in the regime of small dispersion, (ii) does not contain (i) as a special case, since we have not imposed any restriction on the acoustic mismatch between the film and substrate materials. If this mismatch is large, the necessary smallness of the dispersion in (i) is achieved by letting the film thickness be small.

In the following, we shall briefly introduce three methods of deriving an evolution equation for weakly nonlinear and weakly dispersive Rayleigh waves. This equation contains a scalar field that depends on the variables $\xi = x - v_R t$ and a stretched time coordinate $\tau$. ($v_R$ is the phase velocity of linear nondispersive SAWs.) Also, we shall show that the evolution equations derived by these three different approaches are identical.

### A. Projection method

This approach has been pioneered by Reutov [23] and Parker [13–15] for homogeneous substrates and has also been applied to the derivation of nonlinear modulation equations for wave envelopes [24,25]. The displacement field is represented as an asymptotic expansion in powers of a small parameter $0 < \varepsilon \ll 1$ which is of the size of a typical strain:

$$\mathbf{u} = \epsilon \mathbf{u}^{(1)} + \epsilon^2 \mathbf{u}^{(2)} + O(\epsilon^3). \tag{2.7}$$

In addition, the thickness of the film in case (i) or the deviations of the density and elastic moduli from their average values in case (ii) are scaled to be of first order in $\epsilon$, and a stretched time coordinate $\tau = \epsilon t$ is introduced. The field $\mathbf{u}^{(1)}$ must then be a solution of the linearized version of the equations of motion (2.4) and the corresponding boundary conditions. It may be chosen to be a superposition of linear SAWs of the free substrate surface:

$$\mathbf{u}^{(1)}(x,z,t) = \int_0^\infty \frac{dq}{2\pi} e^{iq\xi}\, \mathbf{w}(z|q) A(q,\tau) + \text{c.c.}, \tag{2.8}$$

where c.c. denotes the complex conjugate. $\mathbf{w}$, normalized in an appropriate way, is the displacement field of a straight-crested linear Rayleigh wave with wave vector $(q,0)$. In nonpiezoelectric homogeneous media with a planar surface, it may be represented as the sum of at most three exponentials:

$$\mathbf{w}(z|q) = \sum_{r=1}^{3} \mathbf{b}(r) e^{q\alpha(r)z}. \tag{2.9}$$

In writing Eq. (2.9), we have adopted a normalization that leaves the generalized polarization vectors $\mathbf{b}$ independent of the modulus of $q$. The decay constants $\alpha$ are independent of $|q|$, too.

The field $\mathbf{u}^{(2)}$ is the solution of an inhomogeneous linear boundary value problem. It has to satisfy the equation of motion

$$\left\{ \delta_{\alpha\beta}\rho \frac{\partial^2}{\partial t^2} - \frac{\partial}{\partial x_\mu} C_{\alpha\mu\ \beta\nu} \frac{\partial}{\partial x_\nu} \right\} u_\beta^{(2)} = \frac{1}{2} \frac{\partial}{\partial x_\beta} S_{\alpha\beta\ \mu\nu\ \gamma\delta} u^{(1)}_{\mu,\nu} u^{(1)}_{\gamma,\delta} + 2\rho v_R \frac{\partial^2}{\partial x\, \partial \tau} u_\alpha^{(1)} + L_\alpha \tag{2.10}$$

and boundary condition at $z=0$:

$$-C_{\alpha 3\ \beta\nu} u^{(2)}_{\beta,\nu} = \frac{1}{2} S_{\alpha 3\ \mu\nu\ \gamma\delta} u^{(1)}_{\mu,\nu} u^{(1)}_{\gamma,\delta} + M_\alpha. \tag{2.11}$$

In the case of a thin film coating the substrate [case (i)], the term $L_\alpha$ in the equation of motion vanishes, while

$$M_\alpha = d \left[ \left\{ \delta_{\alpha\beta}\rho_F \frac{\partial^2}{\partial t^2} - g^{(1)}_{\alpha\beta} \frac{\partial^2}{\partial x^2} \right\} u_\beta^{(1)} \right]_{z=0}. \tag{2.12}$$

In the case of $z$-dependent density and/or elastic moduli [case (ii)], these terms have the form

$$L_\alpha = -\Delta\rho v_R^2 u^{(1)}_{\alpha,11} + \frac{\partial}{\partial x_\mu} \Delta C_{\alpha\mu\ \beta\nu} \frac{\partial}{\partial x_\nu} u_\beta^{(1)}, \tag{2.13}$$

$$M_\alpha = \left[ \Delta C_{\alpha 3\ \beta\nu} \frac{\partial}{\partial x_\nu} u_\beta^{(1)} \right]_{z=0}. \tag{2.14}$$

In addition, $\mathbf{u}^{(2)}$ has to decay to zero for $z \to -\infty$ or at least satisfy Sommerfeld-type radiation conditions.

The right-hand sides of Eqs. (2.10) and (2.11) depend on the "fast" variables $x$ and $t$ only through $\xi = x - v_R t$. Since secular terms in $x$ and $t$ have to be avoided, $\mathbf{u}^{(2)}$ can depend on $x$ and $t$ only through $\xi$, too. To ensure that the linear inhomogeneous boundary value problem can be solved without secular terms in $x$ and $t$, a compatibility condition has to be satisfied. This condition is obtained by projecting Eq. (2.10) on a straight-crested surface wave solution

$$\overline{\mathbf{u}}(\xi,z) = e^{iq\xi}\, \mathbf{w}(z|q); \tag{2.15}$$

i.e., Eq. (2.10) is multiplied by $\overline{u}^*_\alpha$, summed over $\alpha = 1,2,3$ and integrated over $x$ from $-\infty$ to $+\infty$ and over $z$ from $-\infty$ to 0. By performing twice an integration by parts and using Eq. (2.11) in the boundary terms, the second-order field $\mathbf{u}^{(2)}$ is eliminated. Transforming from displacement amplitudes $A(q,\tau)$ to strain amplitudes $B(q,\tau) = iqA(q,\tau)$, the following result is obtained, which is the desired evolution equation:

$$i \frac{\partial}{\partial \tau} B(q) = q^2 \Delta(q) B(q) + v_R q \left\{ \int_0^q F(k/q) B(k) B(q-k) \frac{dk}{2\pi} + 2 \int_q^\infty (q/k) F^*(q/k) B(k) B^*(k-q) \frac{dk}{2\pi} \right\} \tag{2.16}$$

for $q > 0$. In Eq. (2.16) and in most of the following equations involving $B$, the dependence on $\tau$ is not indicated explicitly in order to simplify the notation. The quantity $q^2\Delta(q) = \omega(q) - v_R q$ is the difference between the frequency $\omega(q)$ of linear surface waves in the system and Rayleigh waves of a homogeneous substrate with density $\rho$ and second-order elastic moduli $C_{\alpha\beta\ \mu\nu}$ [i.e., the homogeneous substrate without film in case (i) and with $\Delta\rho = 0$, $\Delta C_{\alpha\beta\ \mu\nu}$

$=0$ in case (ii)]. The derivation procedure provides explicit expressions for $\Delta(q)$ in terms of the acoustic properties of the film in case (i), the inhomogeneous parts of the mass density and elastic moduli in case (ii), and the depth profile **w** of linear Rayleigh waves for a homogeneous substrate with no film. These expressions are partly given in Refs. [26,27]. In case (i), $\Delta(q)=v_R\mu_0 d$, where $d$ is the film thickness and the constant $\mu_0$ depends on the ratio of the mass densities of the film and substrate material and on the ratios of the elastic moduli of film and substrate. The coefficient $\mu_0$ can have either sign and may vanish for special choices of the linear acoustic mismatch between film and substrate. This means that the linear dispersion can be normal or anomalous. For isotropic substrates and films, the following simple formula is easily derived:

$$\mu_0 = 0.5 v_R P_0 \left[ \frac{c_F}{c_S} - \frac{\rho_F}{\rho_S} \right], \tag{2.17}$$

where we have defined $c=\lambda+2\mu-\lambda^2/(\lambda+2\mu)$ in terms of the Lamé constants $\lambda$ and $\mu$. The indices $S$ and $F$ stand for substrate and film, respectively. The coefficient

$$P_0 = -2\sqrt{1-(v_R/v_T)^2}\,\frac{c_S}{\mu_S D_0}\left(\frac{v_R}{v_T}\right)^2 \tag{2.18}$$

depends on material constants of the substrate, only. Here,

$$D_0 = 16\left[\frac{1}{4}\left(\frac{v_R}{v_T}\right)^4 + \frac{v_T^4}{v_R^2 v_L^2} + \left(\frac{v_T}{v_R}\right)^2 - 2\left(\frac{v_T}{v_L}\right)^2\right] \tag{2.19}$$

and $v_L$ and $v_T$ are the velocities of the longitudinal and transverse bulk waves in the substrate. $\mu_0$ vanishes if $\rho_F/\rho_S = c_F/c_S$. In this case, we may approximate $\Delta(q)=v_R\mu_1 q d^2$. The following expression is obtained for the coefficient $\mu_1$:

$$\mu_1 = \frac{1}{2}\frac{\rho_F}{\rho_S}\left[P_1 + P_2\frac{\rho_F}{\rho_S} + P_3\frac{\mu_F}{\lambda_F+2\mu_F}\right]. \tag{2.20}$$

Like $P_0$, the coefficients

$$P_1 = \left(\frac{v_R}{v_T}\right)^2\left[2-\left(\frac{v_R}{v_T}\right)^2\right]\frac{c_S}{\mu_S D_0}, \tag{2.21a}$$

$$P_2 = \frac{1}{2D_0}\left(\frac{v_R}{v_T}\right)^4\left[4-\left(\frac{v_R}{v_T}\right)^2\right]\left[\left(\frac{v_R}{v_T}\right)^2 - \frac{c_S}{\mu_S}\right], \tag{2.21b}$$

$$P_3 = -2\left(\frac{v_R}{v_T}\right)^4\left[2-\left(\frac{v_R}{v_T}\right)^2\right]\frac{1}{D_0} \tag{2.21c}$$

depend on the material properties of the substrate only. Depending on the Lamé constants of the film, $\mu_1$ can be positive or negative. It has been reported in Ref. [22] how the asymptotic expansion (2.7) has to be modified in this case to make sure that nonlinearity and linear dispersion appear at the same order in the evolution equation.

The dimensionless function $F$ depends on the ratios of the second-order and third-order elastic moduli of the substrate only. In the above derivations, it results as the overlap integral:

TABLE I. Coefficients $M(r,r',r'')$ (real and imaginary parts), $r,r',r''=1,2$, for the substrate Si(111) and propagation direction $[1\bar{1}2]$. Second-order and third-order elastic moduli taken from Ref. [30]. Normalization: $w_3=1$. The corresponding decay constants $\alpha(r)$, $r=1,2$, are $\alpha(1)=1.202-i0.303$, $\alpha(2)=0.213+i0.079$. Rayleigh wave velocity $v_R=4736$ m/s.

| $(r,r',r'')$ | Re($M$) | Im($M$) |
|---|---|---|
| (1, 1, 1) | 0.335 | 0.312 |
| (1, 1, 2) | −0.295 | −0.070 |
| (1, 2, 1) | −0.295 | −0.070 |
| (1, 2, 2) | 0.309 | 0.120 |
| (2, 1, 1) | −0.441 | 0.041 |
| (2, 1, 2) | 0.369 | −0.155 |
| (2, 2, 1) | 0.369 | −0.155 |
| (2, 2, 2) | −0.390 | 0.025 |

$$F(q'/q) = \frac{-i}{N_0} S_{\alpha\beta\ \mu\nu\ \zeta\xi} \int_{-\infty}^{0} [D_\beta(q) w_\alpha(z|q)]^* \times [D_\nu(q') w_\mu(z|q')][D_\xi(q-q') \times w_\zeta(z|q-q')]\frac{1}{q'(q-q')}dz, \tag{2.22}$$

where

$$N_0 = 4\rho v_R^2 q \int_{-\infty}^{0} w_\alpha^*(z|q) w_\alpha(z|q) dz = 4\rho v_R^2 \sum_{r,r'} \frac{b_\alpha^*(r) b_\alpha(r')}{\alpha^*(r)+\alpha(r')} \tag{2.23}$$

and where we have defined the operator $D_\alpha(q)=iq\delta_{\alpha 1} + \delta_{\alpha 3}\partial/\partial z$. $F$ has the following explicit analytic form:

$$F(X) = \sum_{r,r',r''=1}^{3} \frac{M(r,r',r'')}{\alpha^*(r) + X\alpha(r') + (1-X)\alpha(r'')} \tag{2.24}$$

for arguments $X\in[0,1]$. It obviously has the property $F(X)=F(1-X)$. The coefficients $M(r,r',r'')$ are determined by the formula

$$M(r,r',r'') = \frac{-i}{N_0} S_{\alpha\beta\ \mu\nu\ \zeta\xi} [K_\beta(r) b_\alpha(r)]^* [K_\nu(r') b_\mu(r')] \times [K_\xi(r'') b_\zeta(r'')]. \tag{2.25}$$

The vectors $\mathbf{b}(r)$, $r=1,2,3$, were introduced in Eq. (2.9), and the vectors $\mathbf{K}(r)$ are defined by $K_\alpha(r)=\delta_{\alpha 1} i + \delta_{\alpha 3}\alpha(r)$. Numerical values for these coefficients are listed in Table I pertaining to the (111) surface of silicon with propagation along the $[1\bar{1}2]$ direction.

When calculating these coefficients, the normalization of the functions **w** has been chosen such that $w_3(0|q)=1$. This implies that the Fourier transform of the function $B(q)$ is the local slope of the surface:

$$\int_0^\infty \frac{dq}{2\pi} B(q) e^{iq(x-v_R t)} + \text{c.c.} = u_{3,1}^{(1)}(x,0,t). \tag{2.26}$$

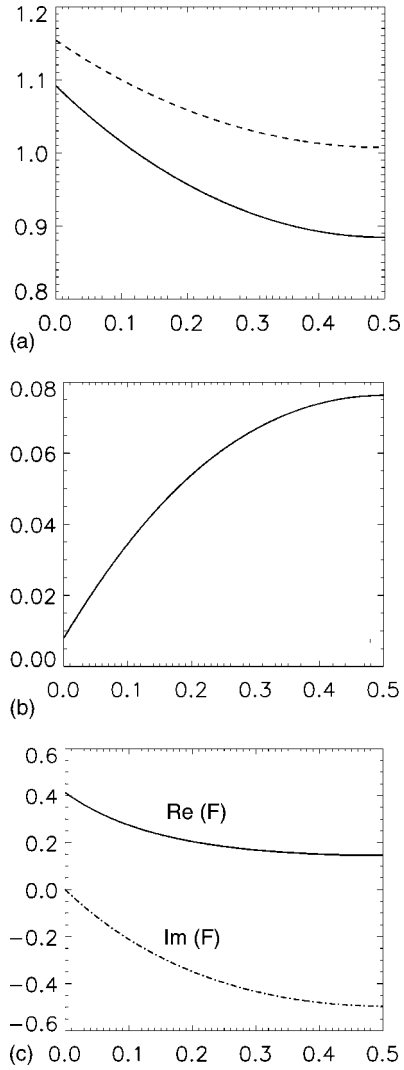


FIG. 1. The dimensionless function $F$ for substrate fused quartz (a), Si(001)⟨001⟩ (b), Si(111)$[11\overline{2}]$ (c). Normalization: $w_1=1$. The second-order and third-order elastic moduli were taken from Ref. [28] [solid line in (a)], Ref. [29] [dashed line in (a)], Ref. [30] [(b),(c)].

In Fig. 1, the function $F(X)$ is shown for three propagation geometries; the first one corresponds to isotropic silica as substrate material, and the other two refer to two different propagation directions and surfaces of silicon. The normalization of $\mathbf{w}$ is now such that $w_1(0|q)=1$, and consequently, the Fourier transform of $B(q)$ is $u_{1,1}^{(1)}(x,0,t)=-v_R\dot{u}_1^{(1)}(x,0,t)$; i.e., it is proportional to the in-plane component of the particle velocity at the surface, a quantity frequently considered in fluid dynamics.

Figure 1 shows that in the isotropic case and for Si(001) with the propagation direction along a cubic axis, the function $F$ is real with the latter normalization (imaginary for the prior normalization). In contrast to these high-symmetry cases, the function $F$ is complex in the case Si(111)⟨112⟩ with the imaginary part being larger than the real part in the latter normalization.

Note that $F(X)$ is proportional to the function $J^{-1}K(X)$, $0<X<1$, which was introduced by Parker [15] and by Parker and David [31]. In the latter work piezoelectricity has also been taken into account. The authors give graphical representations of these functions for two different propagation geometries in the substrate material $LiNbO_3$.

Porubov and Samsonov [32] have described a derivation of an evolution equation for nonlinear SAWs of sagittal polarization propagating in an isotropic substrate coated by an isotropic film. A direct comparison of Eq. (2.16) with their evolution equation [Eq. (4.25) in Ref. [32]] is complicated by the fact that the latter one is not given in explicit form. Their derivation is essentially very similar to the one given in this subsection, also making use of a compatibility condition in its final step. Therefore their evolution equation should agree with Eq. (2.16).

### B. Introduction of a stretched depth coordinate

In the derivation of the evolution equation (2.16) outlined above, the higher-order fields $\mathbf{u}^{(n)}$, $n=2,3,\ldots$, contain secular terms in the depth coordinate $z$. It has been criticized by Lardner [12] that these terms cause the expansion (2.7) to be nonuniform. To avoid such secular terms, he introduced a stretched depth coordinate $\eta=\epsilon z$. The amplitudes of each of the (maximally three) generalized plane waves that make up a straight-crested linear surface wave are allowed to depend on $\eta$ in a different way. Hence, the first-order term in Lardner's asymptotic expansion of the displacement field, $\tilde{\mathbf{u}}=\epsilon\tilde{\mathbf{u}}^{(1)}+\epsilon^2\tilde{\mathbf{u}}^{(2)}+O(\epsilon^3)$, is

$$\tilde{\mathbf{u}}^{(1)}(x,z,t)=\int_0^\infty \frac{dq}{2\pi}e^{iq\xi}\sum_{r=1}^{3}\mathbf{b}(r)e^{q\alpha(r)z}c_r(q,\eta,\tau)+\text{c.c.} \tag{2.27}$$

For $\eta=0$, $\tilde{\mathbf{u}}^{(1)}$ has to satisfy the linearized traction-free boundary conditions at the surface of the substrate. Consequently, $c_r(q,0,\tau)=A(q,\tau)$ is independent of $r$.

In order to exclude secular terms in $z$ from the second-order field $\tilde{\mathbf{u}}^{(2)}$, the following constraints have to be met:

$$\frac{\partial}{\partial\eta}c_r(q,\eta,\tau)=-2ig(r)\frac{\partial}{\partial\tau}c_r(q,\eta,\tau)+iG(r)\times\int_0^q\frac{dk}{2\pi}k(q-k)c_r(k,\eta,\tau)c_r(q-k,\eta,\tau), \tag{2.28}$$

with the coefficients

$$g(r)=\frac{v_R\rho}{n(r)}b_\alpha(r)b_\alpha(r), \tag{2.29}$$

$$G(r)=i\frac{1}{2n(r)}S_{\alpha\beta\,\mu\nu\,\zeta\xi}\,b_\alpha(r)b_\mu(r)b_\zeta(r)K_\beta(r)K_\nu(r)K_\xi(r), \tag{2.30}$$

$$n(r)=b_\alpha(r)\{C_{\alpha3\,\beta\nu}+C_{\alpha\nu\,\beta3}\}K_\nu(r)b_\beta(r). \tag{2.31}$$

These constraints determine the $\eta$ dependence of $c_r(q,\eta,\tau)$, once $c_r(q,0,\tau)=A(q,\tau)$ is known.

At second order of $\epsilon$, the equation of motion in the substrate and the boundary condition at $z=\eta=0$ have the form of Eqs. (2.10) and (2.11) with the following modifications: $\mathbf{u}^{(1)},\mathbf{u}^{(2)}$ have to be replaced by $\tilde{\mathbf{u}}^{(1)},\tilde{\mathbf{u}}^{(2)}$, to the right-hand side of Eq. (2.10) one has to add $\{C_{\alpha 3\ \beta\nu}+C_{\alpha\nu\ \beta 3}\}\times(\partial/\partial\eta)\tilde{u}^{(1)}_{\beta,\nu}$, and the right-hand side of the boundary condition Eq. (2.11) has to be supplemented by the term $C_{\alpha 3\ \beta 3}(\partial/\partial\eta)\tilde{u}^{(1)}_{\beta}$. All terms in Eq. (2.11) have to be taken at $z=\eta=0$.

Due to the additional terms, the linear inhomogeneous boundary value problem for $\tilde{\mathbf{u}}^{(2)}$ at $\eta=0$ differs from the corresponding one for $\mathbf{u}^{(2)}$. However, the compatibility conditions of both boundary value problems, which constitute the evolution equation for $A(q,\tau)$, turn out to be identical. This can be easily shown by projecting the equation of motion for $\tilde{\mathbf{u}}^{(2)}$ on $\bar{\mathbf{u}}$ as defined in Eq. (2.15) and integrating by parts in the same fashion as done when deriving the evolution equation (2.16) in the previous subsection. As a result, Eq. (2.16) is obtained with the following additional terms on the right-hand side:

$$\frac{-2iq}{N_0}\left\{\int_{-\infty}^{0} w^*_\alpha(z|q)\{C_{\alpha 3\ \beta\nu}+C_{\alpha\nu\ \beta 3}\}q \times\sum_{r=1}^{3}K_\nu(r)b_\beta(r)e^{q\alpha(r)z}\left[\frac{\partial}{\partial\eta}c_r(q,\eta,\tau)\right]_{\eta=0}dz - w^*_\alpha(0|q)C_{\alpha 3\ \beta 3}\sum_{r=1}^{3}b_\beta(r)\left[\frac{\partial}{\partial\eta}c_r(q,\eta,\tau)\right]_{\eta=0}\right\}. \tag{2.32}$$

The expression (2.32) vanishes, as can be shown by considering the identities

$$\begin{aligned}0&=\int_{-\infty}^{0} zf_\alpha(z)\{(v_Rq)^2\delta_{\alpha\beta}+D_\mu(q)C_{\alpha\mu\ \beta\nu}D_\nu(q)\}w^*_\beta(z|q)dz\\ &=\int_{-\infty}^{0} w^*_\alpha(z|q)\{(v_Rq)^2\delta_{\alpha\beta}+D_\mu(q)C_{\alpha\mu\ \beta\nu}D_\nu(q)\}zf_\beta(z)dz\\ &\quad-w^*_\alpha(0|q)C_{\alpha 3\ \beta 3}f_\beta(0)=\int_{-\infty}^{0} w^*_\alpha(z|q)\{C_{\alpha 3\ \beta\nu}\\ &\quad+C_{\alpha\nu\ \beta 3}\}D_\nu(q)f_\beta(z)-w^*_\alpha(0|q)C_{\alpha 3\ \beta 3}f_\beta(0),\end{aligned} \tag{2.33}$$

where we have used the abbreviation

$$\mathbf{f}(z)=\sum_{r=1}^{3}\mathbf{b}(r)e^{q\alpha(r)z}\left[\frac{\partial}{\partial\eta}c_r(q,\eta,\tau)\right]_{\eta=0}. \tag{2.34}$$

### C. Hamiltonian approach

This alternative method of deriving the evolution equation for weakly nonlinear SAWs has been used extensively by Zabolotskaya and co-workers to describe nonlinear Rayleigh, Stoneley, and Scholte waves [16–18,33]. It is summarized here in a simplified form without introducing explicitly conjugate momenta and the canonical equations. An exact solution of the linearized equation of motion and boundary condition in the form of a superposition of straight-crested SAWs,

$$\mathbf{u}(x,z,t)=\int_{-\infty}^{\infty}\frac{dq}{2\pi}\tilde{\mathbf{w}}(z|q)e^{iqx}a(q,t), \tag{2.35}$$

is inserted into the Lagrangian (2.1), which leads to an effective Lagrangian for the amplitudes $a(q)$:

$$\begin{aligned}L=\int_{-\infty}^{d}dz\Bigg\{&\int_{-\infty}^{\infty}\frac{dq}{2\pi}\frac{1}{2}\rho(z)\tilde{w}_\alpha(z|-q)\tilde{w}_\alpha(z|q)\dot{a}(-q)\dot{a}(q)\\ &-\int_{-\infty}^{\infty}\frac{dq}{2\pi}\frac{1}{2}C_{\alpha\mu\ \beta\nu}(z)[D_\mu(-q)\tilde{w}_\alpha(z|-q)]\\ &\times[D_\nu(q)\tilde{w}_\beta(z|q)]a(-q)a(q)\\ &-\int_{-\infty}^{\infty}\frac{dq}{2\pi}\int_{-\infty}^{\infty}\frac{dk}{2\pi}\int_{-\infty}^{\infty}\frac{dp}{2\pi}\frac{1}{6}S_{\alpha\beta\ \mu\nu\ \zeta\xi}(z)[D_\beta(q)\tilde{w}_\alpha(z|q)]\\ &\times[D_\nu(k)\tilde{w}_\mu(z|k)][D_\xi(p)\tilde{w}_\zeta(z|p)]\\ &\times2\pi\delta(q+k+p)a(q)a(k)a(p)\Bigg\}.\end{aligned} \tag{2.36}$$

We emphasize that $\tilde{\mathbf{w}}(z|q)$ is the depth profile of a linear SAW propagating in the substrate covered with a thin film and/or having $z$-dependent material properties. Furthermore $\tilde{\mathbf{w}}(z|-q)=\tilde{\mathbf{w}}^*(z|q)$ and $a(-q,t)=a^*(q,t)$. The second term on the right-hand side of Eq. (2.36) is now integrated by parts taking advantage of the fact that

$$C_{\alpha 3\ \mu\nu}(d)[D_\nu(q)\tilde{w}_\mu(z|q)]_{z=d}=0. \tag{2.37}$$

Performing now the variation of the action integral with respect to the real and imaginary parts of the complex amplitudes $a(q)$, $q>0$ or, equivalently, with respect to $a(-q)$, $q>0$, one obtains equations of motion for the amplitudes $a(q)$:

$$\begin{aligned}0=\int_{-\infty}^{d}dz\Bigg\{&\rho(z)\tilde{w}_\alpha(z|-q)\tilde{w}_\alpha(z|q)\ddot{a}(q)-\tilde{w}_\alpha(z|-q)\\ &\times D_\mu(q)C_{\alpha\mu\ \beta\nu}(z)D_\nu(q)\tilde{w}_\beta(z|q)a(q)\\ &+\frac{1}{2}S_{\alpha\beta\ \mu\nu\ \zeta\xi}(z)\int_{-\infty}^{\infty}\frac{dk}{2\pi}[D_\beta(-q)\tilde{w}_\alpha(z|-q)][D_\nu(k)\tilde{w}_\mu(z|k)]\\ &\times[D_\xi(q-k)\tilde{w}_\zeta(z|q-k)]a(k)a(q-k)\Bigg\}.\end{aligned} \tag{2.38}$$

Decomposing now the complex amplitude $a(q,t)$ into a part that varies slowly and one that varies rapidly in time,

$$a(q,t)=A(q,t)\exp(-iv_Rqt), \tag{2.39}$$

and neglecting the second time derivative of $A$, Eq. (2.38) becomes

$$\frac{\partial}{\partial t}A(q) = \frac{1}{2qv_R}[\omega^2(q) - (v_R q)^2]A(q) + \int_{-\infty}^{\infty}\frac{dk}{2\pi}G(q,k)A(k)A(q-k), \quad (2.40)$$

where $\omega(q)$ is the frequency of the linear surface wave with wave number $q$, propagating in the layered and/or inhomogeneous substrate, while

$$G(q,k) = \frac{1}{N(q)}\int_{-\infty}^{d} dz\; S_{\alpha\beta\;\mu\nu\;\zeta\xi}(z)[D_\beta(-q)\tilde{w}_\alpha(z|-q)] \times [D_\nu(k)\tilde{w}_\mu(z|k)][D_\xi(q-k)\tilde{w}_\zeta(z|q-k)] \quad (2.41)$$

and

$$N(q) = 4v_R|q|\int_{-\infty}^{d} dz\; \rho(z)\tilde{w}_\alpha^*(z|q)\tilde{w}_\alpha(z|q). \quad (2.42)$$

Since the dispersion is small, $|\omega^2(q)-(v_R q)^2| \ll (v_R q)^2$, we may replace $\omega^2(q)-(v_R q)^2$ by $2v_R q^3\Delta(q)$ in Eq. (2.40). In addition, the integrals over $z$ in Eqs. (2.41) and (2.42) may be extended from $-\infty$ to 0 and $\tilde{\mathbf{w}}$ may be replaced by $\mathbf{w}$. Also $S(z)$ and $\rho(z)$ may be replaced by their average values $\overline{S}$ and $\overline{\rho}$ in the latter two equations. In this way, the evolution equation (2.16) is recovered with the same expression (2.22) for the function $F$. The equivalence of this Hamiltonian approach and the one introduced in the first subsection has already been stated by Reutov [23] for the nondispersive case.

The factorization (2.39) may already be done in the Lagrangian (2.36). Neglecting there $\dot{A}(q)\dot{A}(-q)$ in comparison to $|v_R q A(q)\dot{A}(-q)|$ and introducing the approximations stated below Eq. (2.42), a Lagrangian for the evolution equation (2.16) is obtained:

$$\mathcal{L} = \int_{-\infty}^{\infty}\frac{dq}{2\pi}\mathrm{sgn}(q)\left\{\frac{1}{q^2}i\left[B(-q)\frac{\partial}{\partial\tau}B(q) - B(q)\frac{\partial}{\partial\tau}B(-q)\right] - 2\Delta(|q|)B(-q)B(q)\right\} - \int_{-\infty}^{\infty}\frac{dq}{2\pi}\int_{-\infty}^{\infty}\frac{dk}{2\pi}\int_{-\infty}^{\infty}\frac{dp}{2\pi} \times K(q,k,p)2\pi\delta(q+k+p)B(q)B(k)B(p), \quad (2.43)$$

with the function

$$K(q,k,p) = \frac{4iv_R}{3N_0 qkp}S_{\alpha\beta\;\mu\nu\;\zeta\xi}\int_{-\infty}^{0}[D_\beta(q)w_\alpha(z|q)] \times [D_\nu(k)w_\mu(z|k)][D_\xi(p)w_\zeta(z|p)]dz, \quad (2.44)$$

which is symmetric with respect to permutations of its arguments. For $0<k<q$, the relation $K(-q,k,q-k) = 4v_R F(k/q)/(3q)$ holds. It is easy to verify that variation of the action integral with the Lagrangian (2.43) leads to Eq. (2.16) [34]. Applying Noether's theorem to translational invariance of the Lagrangian in space and time, the following two conserved quantities are obtained:

$$\int_0^{\infty}\frac{dq}{2\pi}\frac{1}{q}|B(q)|^2, \quad (2.45)$$

$$\int_0^{\infty}\frac{dq}{2\pi}\frac{i}{q^2}\left\{B^*(q)\frac{\partial}{\partial\tau}B(q) - B(q)\frac{\partial}{\partial\tau}B^*(q)\right\}. \quad (2.46)$$

### D. Other evolution equations

When transforming Eq. (2.16) from Fourier space into real space, the nonlinearity in the evolution equation will reveal its strongly nonlocal character. This is in particular due to the factor $q/k$ in the second nonlinear term of Eq. (2.16). In this respect, Eq. (2.16) differs from the KdV equation and the Benjamin-Ono equation which have both been suggested as governing equations for nonlinear SAWs [35–38].

Gusev *et al.* [39,40] have developed an evolution equation for nonlinear Rayleigh waves in homogeneous half-spaces which contains a nonlocal second-order nonlinearity expressed in terms of Hilbert transforms. This equation has been used to interpret recent SAW experiments. In a regime far from shock formation, very satisfactory agreement has been found between experimental wave form evolution and theoretial predictions based on this evolution equation [41–43]. However, this equation differs from Eq. (2.16). (For a discussion of the differences see also Ref. [33].) The approach of Gusev *et al.* has also been extended to include dispersion of acoustic waves, and solitary wave solutions have been discussed for special cases [62].

In the derivations of the evolution equation (2.16) outlined above, we had in view the temporal evolution of an initial wave profile. The strain field at the surface is therefore a function of the coordinate $\xi = x - v_R t$ and the stretched time $\tau$. Equally, one may consider the spatial evolution (in the $x$ direction along the surface) of a temporal strain pulse, for example. This viewpoint pertains to the experiments described in Sec. IV. In this case, one obtains the same evolution equation (2.16), where $\tau$ is now interpreted as a stretched spatial coordinate. More precisely, $\tau = \epsilon x/V_x$, where $V_x$ is the $x$ component of the group velocity associated with nondispersive linear Rayleigh waves propagating in the $x$ direction of the substrate's surface. This is easily shown by using the projection method.

## III. TRAVELING WAVE SOLUTIONS

When assuming for the linear dispersion the power law $q^2\Delta(q) = \overline{\mu}_{\ell-2}q^\ell$, $\ell \geqslant 2$, and inserting into Eq. (2.16) the ansatz

$$B(q,\tau) = \kappa^{s_1}Q(\kappa^{s_2}q)e^{\mp iq\kappa v_R\tau} \quad (3.1)$$

for the dependence of $B$ on $\tau$ and $q$ with $\kappa > 0$, $s_1 = (\ell-2)/(\ell-1)$, and $s_2 = -1/(\ell-1)$, the following integral equation is obtained:

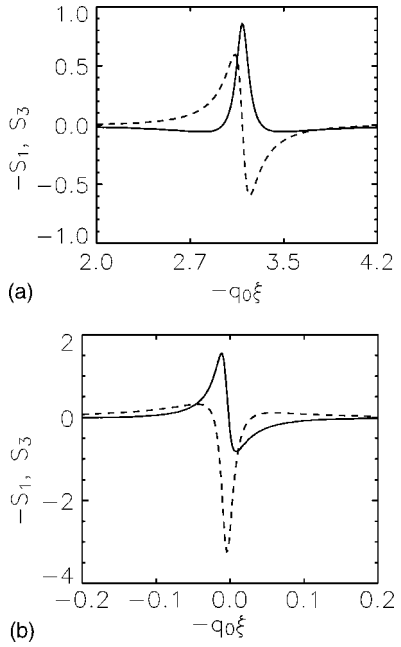


FIG. 2. Solitary pulse shapes for the substrate Si(001)⟨001⟩ (a), Si(111)$[\overline{112}]$ (b). Solid line: $-S_1$. Dashed line: $S_3$ (rescaled).

$$[\pm 1 + q^{\ell-1}Z_\ell]Q(q) = \int_0^q F(k/q)Q(k)Q(q-k)\frac{dk}{2\pi} + 2\int_q^\infty (q/k)F^*(q/k)Q(k)Q^*(k-q)\frac{dk}{2\pi}, \tag{3.2}$$

where $Z_\ell = -\overline{\mu}_{\ell-2}/v_R$. From Eq. (3.2) we may deduce that if a solitary solution exists for these dispersion laws, it will obey the scaling

$$u^{(1)}_{\alpha,1}(x,0,t) = \kappa S_\alpha(\kappa^{1/(\ell-1)}(\xi \mp \kappa v_R \tau - \xi_0)). \tag{3.3}$$

For more general dispersion laws that are not power laws, one may still find solitary solutions with an ansatz of the form (3.1), but the scaling property (3.3) is no longer present. The function $S_\alpha$ represents the shape of the solitary solution. For an isotropic substrate, $S_1$ is even and $S_3$ is odd, which is related to the fact that $F$ is purely real (purely imaginary) for $Q$ being the Fourier transform of $S_1$ ($S_3$). In general, $S_1$ and $S_3$ are related to each other via

$$S_3(\xi) = c_1\hat{H}[S_1](\xi) + c_2 S_1(\xi) + O(\epsilon). \tag{3.4}$$

with the coefficients $c_1$ and $c_2$ that are determined by the linear acoustic properties of the (homogeneous) substrate. ($\hat{H}[S]$ is the Hilbert transform of $S$.) These functions can be determined numerically as a limiting case of stationary periodic solutions with periodicity $\Lambda = 2\pi/q_0$. With $B(q,\tau) = 2\pi\delta(q-nq_0)\kappa Q_n \exp(\mp i n q_0 \kappa v_R \tau)$ in Eq. (2.16) and by limiting the number of harmonics to $N$, the integral equation (3.2) is converted into a set of $N$ nonlinear coupled algebraic equations:

$$(\pm 1 + \zeta_\ell n^{\ell-1})Q_n = \sum_{m=1}^{n-1} F(m/n)Q_m Q_{n-m} + 2\sum_{m=n+1}^{N} (n/m)F^*(n/m)Q_m Q^*_{m-n}, \tag{3.5}$$

where $\zeta_\ell = Z_\ell q_0^{\ell-1}/\kappa$. For given values of $\zeta_\ell$ and $N$, Eq. (3.5) is solved numerically with the help of a Newton-Raphson minimization routine. With decreasing $|\zeta_\ell|$ the periodic wave form resulting from the solution of Eq. (3.5) becomes a periodic pulse train with well-separated pulses.

In Fig. 2, pulse shapes are compared for two propagation geometries pertaining to the same substrate material—namely, silicon. In the first case Si(001)⟨100⟩, $S_1$ is an even and $S_3$ is an odd function as in isotropic substrates. In the second case Si(111)$[\overline{112}]$, the pulse shapes are no longer purely even or purely odd. In addition, the shapes of $S_1$ and $S_3$ seem to be nearly reversed as compared to the first case: $S_1$ is almost antisymmetric while $S_3$ is almost symmetric. This is a strong manifestation of the substrate's anisotropy.

A characteristic feature of $S_1$ in isotropic substrates and for Si(001)⟨100⟩ as well as $S_3$ for Si(111)⟨$11\overline{2}$⟩ is the "Mexican hat" shape. The appearance of the two negative minima next to the maximum is forced upon the pulse by the condition that the integral over the pulse has to vanish:

$$\int_{-\infty}^{\infty} S_\alpha(\xi)d\xi = 0. \tag{3.6}$$

This is a direct consequence of the factor $q/k$ in the second nonlinear term on the left-hand side of the integral equation (3.2). Since the function $F$ is bounded, this causes the behavior $Q(q) \to 0$ as $q \to 0$.

Once a stationary solution $S_\alpha$ is found for a given dispersion parameter $\overline{\mu}_{\ell-2} < 0$ (normal dispersion), the corresponding solution for the same value of $\overline{\mu}_{\ell-2}$, but with reversed sign (anomalous dispersion), is also found:

$$u^{(1)}_{\alpha,1}(x,0,t) = -\kappa S_\alpha(\kappa^{1/(\ell-1)}(\xi \pm \kappa v_R \tau - \xi_0)). \tag{3.7}$$

The sign change of the solitary wave and of its velocity relative to $v_R$ has been confirmed in recent experiments [6]. In all cases that we have investigated, the solitary pulses propagate faster than nondispersive Rayleigh waves in the case of normal dispersion and slower for anomalous dispersion.

Another interesting aspect is the transformation property of the solitary pulse under inversion of the propagation direction. Defining $\overline{\xi} = x + v_R t$ and choosing

$$\mathbf{u}^{(1)}(x,z,t) = \int_0^\infty \frac{dq}{2\pi} e^{iq\overline{\xi}}\, \mathbf{w}(z|q)\overline{B}(q,\tau)/(iq) + \text{c.c.}, \tag{3.8}$$

instead of Eq. (2.8) in the asymptotic expansion (2.7), we obtain for the strain amplitudes $\overline{B}(q,\tau)$ an evolution equation that differs from Eq. (2.16) only by the sign of its left-hand side. [Note that the right-hand side of Eq. (3.8) solves the

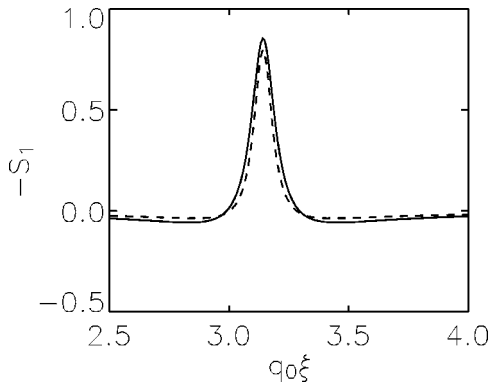


FIG. 3. Solitary pulse shape for Si(001)⟨001⟩ determined with the complete function $F$ (solid line) and with $F(X)$ approximated by $F(1/2)$ (dashed line).

linearized equation of motion and boundary conditions for a homogeneous substrate in the absence of a film.] Consequently, the ansatz

$$\overline{B}(q,\tau) = \kappa^{s_1} Q(\kappa^{s_2} q) e^{\pm iq\kappa v_R \tau} \tag{3.9}$$

instead of Eq. (3.1) leads again to Eq. (3.2) for the Fourier transform of the pulse shape, $Q(q)$. This leads us to the following conclusion: If Eq. (3.3) is a pulse solution propagating in the positive $x$ direction, then

$$u^{(1)}_{\alpha,1}(x,0,t) = \kappa S_\alpha(\kappa^{1/(\ell-1)}(\overline{\xi} + \kappa v_R \tau - \overline{\xi}_0)) \tag{3.10}$$

is the corresponding pulse solution propagating in the negative $x$ direction. This also follows directly from the time reversal symmetry of the equations of elasticity theory. Rotating now the coordinate system around the $z$ axis such that the direction of the $x$ axis is reversed, we obtain the following transformation formulas for the pulse shape functions: $S_1(x) \to S_1(-x)$, $S_3(x) \to -S_3(-x)$. In isotropic substrates, $S_1$ is an even function and $S_3$ is an odd function. Consequently the pulse shapes are unchanged when reversing the propagation direction. More generally this holds true whenever the function $F$ is purely real for the normalization $w_1 = 1$ and purely imaginary for the normalization $w_3 = 1$. If this is not the case, as in the substrate geometry Si(111)⟨112⟩, the pulse shapes may strongly change when reversing the propagation direction. This is a remarkable effect of anisotropy, which was verified experimentally for silicon.

The detailed behavior of the function $F$ in the nonlinear terms of the evolution equation seems to have only a minor influence on the solitary pulse shapes, especially for fused quartz as substrate material, where $F(X)$ varies little with $X$ (by ≈20%). In the case of the Si(001) substrate with propagation along the ⟨100⟩ direction, the function $F(X)$ does show considerable variation, as its value at $X = 0$ is only 10% of $F(1/2)$. But even here, the pulse profiles determined with the full $F$ and with $F(X)$ replaced by $F(1/2)$ differ very little (Fig. 3). Therefore, we may expect that replacing $F(X)$ in Eq. (2.16) by the constant $F(1/2)$ will yield a reasonable approximation for the pulse shapes as well as for the dynamics in many propagation geometries. In the absence of dispersion, the evolution equation with this replacement is identical to the approximate equation (16) with Eq. (15) [or Eq. (38)] in Ref. [44]. Recently, this equation has also been found in the context of magnetohydrodynamics [45], and it has been derived for weakly guided nonlinear Scholte waves [46]. In the context of SAWs, the approximation $F(X) = \text{const}$ becomes exact in the special case of one-component surface waves [47]. However, care has to be taken in the case of a coated substrate, since a thin film may cause the one-component surface wave to become leaky. We emphasize that when transforming Eq. (2.16) into real space, its nonlinearity remains highly nonlocal even with this approximation. This is due to the factor $q/k$ in the second nonlinear term.

For the special situation of a dispersion term of the form $\overline{\mu}_1 q^3$ discussed in the previous section (a KdV-type dispersion), closed-form expressions are known for a two-parameter family of solitary wave solutions (parameters $\kappa$ and $\xi_0$) and a three-parameter family of stationary periodic solutions (parameters $\kappa$, $\xi_0$, and the periodicity $\Lambda = 2\pi/q_0$) of the evolution equation (2.16) with constant $F(X) = F_0$. In the following, we assume this constant to be real without loss of generality. [If $F(1/2)$ is complex, it can be made real by a simple transformation of the phases of the complex amplitudes $B(q)$.] The resulting analytic solution is found with the simple ansatz $Q(q) = \gamma q \exp(-q\beta)$. A simplification is achieved by a transition from strain amplitudes $B(q)$ to the displacement amplitudes $A(q)$ with $B(q) = |q|A(q)$. The evolution equation then takes the form

$$i\frac{\partial}{\partial \tau}A(q) = \overline{\mu}_1 q^3 A(q) + v_R F_0 \left\{ \int_0^q k(q-k)A(k)A(q-k)\frac{dk}{2\pi} + 2\int_q^\infty q(k-q)A(k)A^*(k-q)\frac{dk}{2\pi} \right\}. \tag{3.11}$$

If $B(q)$ is the Fourier transform of $u^{(1)}_{1,1}(x,0,t)$ in the case of an isotropic substrate, $A(q)$ is proportional to the Fourier transform of the surface elevation profile $U(\xi,\tau) = u^{(1)}_3(x,0,t)$. The ansatz $A(q,\tau) = \gamma \exp(-q[\beta + i\kappa v_R \tau])$ solves Eq. (3.11), if

$$\gamma = 12\pi Z_3 / F_0 \tag{3.12}$$

and

$$\beta^2 = 3Z_3/\kappa. \tag{3.13}$$

The corresponding surface elevation profile has Lorentzian form

$$U(\xi,\tau) = \frac{\beta\gamma/\pi}{(\xi - \kappa v_R \tau)^2 + \beta^2}. \tag{3.14}$$

The in-plane component of the particle velocity at the surface, $\dot{u}^{(1)}_1(x,0,t)$, has the characteristic "Mexican hat" shape. Stationary periodic solutions are found via $A(q,\tau) = 2\pi\delta(q - nq_0)\overline{\gamma}\exp(-n[\overline{\beta} + iq_0\kappa v_R\tau])$, where $\overline{\gamma} = 6Z_3 q_0/F_0$ and $3\sinh^{-2}\overline{\beta} = 1 + \kappa/(Z_3 q_0^2)$. The real-space version of this solution is

$$U(\xi,\tau)=\overline{\gamma}\left[\frac{\sqrt{1-b^2}}{1-b\,\cos[q_0(\xi-\kappa v_R\tau)]}-1\right], \quad (3.15)$$

where $b=\mathrm{sech}\overline{\beta}$. Equations (3.14) and (3.15) are almost identical to the corresponding solutions of the Benjamin-Ono equation [48]. However, the relation between width, height, and velocity differs. Nevertheless, Eq. (3.11) shares with the Benjamin-Ono, KdV, and other evolution equations the property that its stationary periodic solution may be expressed as a linear superposition of localized pulses having the same shape and the same relation between height and width as the one-solitary-wave solution. This follows from the fact that

$$\frac{\sqrt{1-b^2}}{1-b\,\cos(q_0\xi)}=2|y_p|\sum_{n=-\infty}^{\infty}\frac{1}{(q_0\xi-2n\pi)^2+y_p^2}+\text{const}, \quad (3.16)$$

where $\cosh(y_p)=1/b$.

Remarkably, the solitary wave solution (3.14) exhibits algebraic decay while the linear limit of the evolution equation (3.11), having KdV-type dispersion, suggests exponential decay. However, because of the nonlocality of the nonlinearity in real space, the linear limit is not relevant for the tails of the solitary pulse.

So far, we have not been able to find closed-form expressions for the solitary pulses in the experimentally most relevant case of a dispersion term $\overline{\mu}_0 q^2 A(q)$, and it does not seem to be straightforward to generalize the above ansatz to construct analogous analytic solutions for other special dispersion laws of polynomial form.

## IV. EXCITATION AND OBSERVATION OF SOLITARY PULSES

The excitation and detection of the solitary SAW pulses was performed with a contact-free all-optical technique. Details concerning the physical background of this experimental method can be found in Ref. [27]. The technique has also been used efficiently in other contexts of acoustic waves in solids. A very recent example is an investigation of ultrasonic wave propagation in heterogeneous rock samples [49].

The straight-crested surface pulses were excited with a *Q*-switched Nd:YAG laser, operated at 1.064 $\mu$m, by focusing the 8-ns-long laser pulses, with 30–60 mJ pulse energy, to a line of 7 mm length and about 30 $\mu$m width with a cylindrical lens. To excite sufficiently nonlinear SAW pulses a highly absorbing thin layer of a carbon suspension was deposited in the source region, which completely absorbed the laser radiation. The explosive evaporation of this layer and the resulting recoil momentum exert a high pressure normal to the surface and launch a strongly nonlinear surface pulse [5,6]. With this technique Mach numbers in the range of about 0.01 have been achieved, limited by the fracture strength of the material [50]. The excitation-detection setup had a bandwidth of about 500 MHz.

The evolution of the propagating SAW pulse profile was registered at two locations, separated by a few millimeters to centimeters from the line source, using a probe-beam-deflection setup. As probe laser a frequency-doubled diode-pumped cw Nd:YAG laser with 100 mW power at 532 nm was employed. The output signal of the position-sensitive detector is proportional to the slope $u_{3,1}=\partial u_3/\partial x$ at the free surface. As in the previous sections, $u_3$ is the normal surface displacement and the wave propagates along the $x$ axis. The surface slope is related to the normal component of the particle velocity at the surface, $u_{3,1}=-\dot{u}_3/v_R+O(\epsilon^2)$. Note that the longitudinal or in-plane component $u_{1,1}$ of the SAW pulse could not be measured.

For a comparison between experiment and theory the two-point-probe detection is crucial. This comparison is performed with the help of numerical simulations on the basis of the evolution equation (2.16). In our numerical scheme, the Fourier transform of the surface slope is discretized, $B(q,\tau)=2\pi\delta(q-nq_0)B_n(\tau)$; i.e., the Fourier integral (2.26) is replaced by a Fourier series with an assumed periodicity $T=2\pi/(q_0 v_R)$. Its value is chosen sufficiently large such that it does not influence the results. The Fourier series is truncated at $n=N$ with $N$ chosen sufficiently large to properly resolve the pulse shape at the first observation point and features emerging in the course of the pulse evolution. In this way, evolution equation (2.16) is then reduced to a set of $N$ coupled complex nonlinear ordinary differential equations:

$$i\frac{\partial}{\partial\tau}B_n=n^2q_0^2\Delta(nq_0)B_n+v_R nq_0\left\{\sum_{m=1}^{n-1}F(m/n)B_mB_{n-m}+2\sum_{m=n+1}^{N}(n/m)F^*(n/m)B_mB_{m-n}^*\right\}, \quad (4.1)$$

which have been integrated numerically.

The wave form detected at the first probe location ($x=0$) is multiplied by a calibration factor and expanded into a Fourier series

$$u_{3,1}(0,0,t)=\sum_{n=1}^{N}\epsilon B_n(0)e^{-inq_0v_Rt}+\text{c.c.} \quad (4.2)$$

The evolution of the Fourier amplitudes $B_n(\tau)$ from the first to the second probe location ($x=x_2$) is determined by integrating Eq. (4.1) from $\tau=0$ to $\tau=\epsilon x_2$, using a predictor-corrector method with variable step size. Summing up the Fourier series with the amplitudes $B_n(\epsilon x_2)$, the simulated surface slope $u_{3,1}(x_2,0,t)$ at the second probe location is obtained and compared with the experimental pulse shape. Experimental and simulation results are shown in Fig. 4 for a strain pulse propagating on a silicon substrate [(111) surface] in the $[\overline{1}12]$ direction. The substrate was covered with a silicon oxide film. The second probe location had a distance of 15.5 mm from the first one. The pulse shapes at the first and second probe locations may be compared with the stationary solitary wave solution shown in Fig. 2(b). The lower inset of Fig. 4 shows that the solitary pulse has already largely formed at the first probe location. The asymmetry of the solitary pulse with the maximum on the left is consistently found in the experiment, in the simulation and in the stationary solution of the evolution equation [Fig. 2(b)]. The simulation extends to distances far beyond the second probe lo-

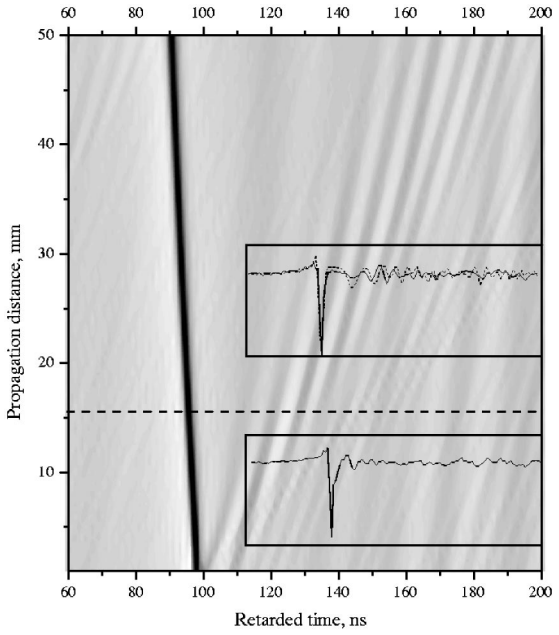


FIG. 4. Evolution of a strain pulse, generated by laser excitation on a Si(111) surface coated with a silicon oxide film. Propagation direction: $[\overline{1}12]$ The local surface slope $u_{3,1}$ is shown. Gray scale: result of numerical simulation with experimental pulse at the first probe location as initial condition. (Dark: negative. Bright: positive values of $u_{3,1}$.) Lower inset: experimental pulse shape at the first probe location. Upper inset: experimental (solid line) and simulated (dashed line) pulse shape at the second probe location. Position of the second probe indicated by a horizontal dashed line.

cation and reveals a stable propagation of the solitary pulse without a visible change of its shape. In addition, radiation is found that is generated in the course of the formation of the solitary pulse and that propagates at a velocity smaller than the solitary pulse. Due to normal linear dispersion, the radiation is slower than $v_R$ while the solitary pulse propagates at a velocity larger than $v_R$ and consequently arrives at the second probe earlier than the radiation.

To realize normal dispersion a film is needed which loads the substrate. For example, a NiCr (80% Ni, 20% Cr) film of 300 nm thickness on fused silica or a 110-nm-thick silicon oxide film on crystalline silicon generated a single solitary pulse at the remote probe location. On the other hand, a stiffening film is needed to obtain an anomalous dispersion effect. This case was realized by deposition of a 50-nm-thick titanium-nitride film on fused silica. The normal and anomalous dispersion was matched with the nonlinearity to generate solitary surface elastic pulses [6].

## V. PULSE COLLISIONS

The pulse dynamics has been investigated numerically in the way described in the previous section imposing periodic boundary conditions in the $\xi$ domain. The system of $N$ coupled nonlinear ordinary differential equations corresponding to Eq. (4.1) was integrated using a variable-step-size Adams method (see, for example, Ref. [51]). In our numerical studies of pulse collisions, the following initial conditions were chosen:

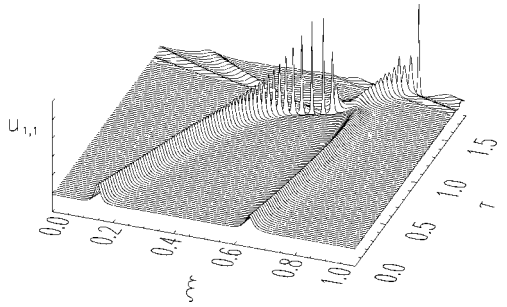

FIG. 5. Collision of solitary pulses: BO-type linear dispersion, $F$ approximated by a constant. (In this and the following figures, the units at the axes are arbitrary.)

$$B_n(0) = \kappa_I Q_n^{(I)} + \exp(in\phi)\kappa_{II} Q_n^{(II)}. \tag{5.1}$$

Here, $Q_n^{(I)}$ and $Q_n^{(II)}$ are solutions of Eq. (3.5), with $\zeta_\ell = -\overline{\mu}_{\ell-2} q_0^{\ell-1}/(\kappa_I v_R)$ and $\zeta_\ell = -\overline{\mu}_{\ell-2} q_0^{\ell-1}/(\kappa_{II} v_R)$, respectively. They correspond to pulse trains with well-separated highly localized pulses. The phase angle $\phi$ is chosen such that the two pulse trains do not overlap.

Two types of linear dispersion laws were considered in the numerical pulse collision simulations: (i) $q^2\Delta(q) \propto q^2$, which is the usual situation for a thin film on a homogeneous substrate. The linear dispersion term in the evolution equation is then the same as the one in the BO equation. (ii) $q^2\Delta(q) \propto q^3$, which corresponds to a special choice of the acoustic mismatch between film and substrate, as pointed out in Sec. II A. In this case, the linear dispersion term is identical to that in the KdV equation.

A typical scenario for pulse collisions in the case of BO-type dispersion is shown in Fig. 5. In this simulation, the function $F$ was approximated by a constant. When the two pulses approach each other, the faster of the two is accelerated and thereby further compressed. The collision is strongly inelastic. A similar behavior was found for the function $F$ corresponding to Si(001)⟨100⟩ [52]. In another example pertaining to an isotropic substrate [53], the acceleration of the faster pulse was not very pronounced. In all three cases, the following features were observed: The two pulses do not really pass through each other. The compression of

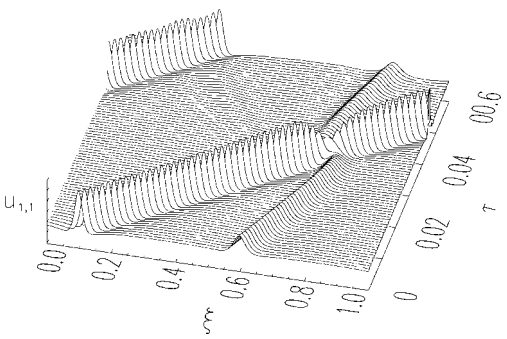

FIG. 6. Collision of solitary pulses: KdV-type linear dispersion, $F$ approximated by a constant.

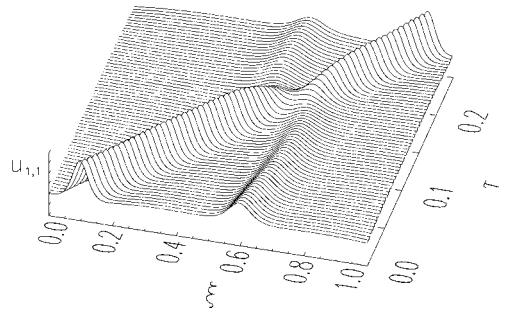


FIG. 7. Collision of solitary pulses: KdV-type linear dispersion, $F$ corresponding to fused silica as substrate material.

the faster pulse continues after the collision, and the slower pulse seems to be converted into radiation—i.e., into quasilinear waves.

The situation is completely different in the case of KdV-type linear dispersion as demonstrated in Fig. 6. Here, the pulse collision is nearly elastic with only a small amount of radiation being generated. An almost elastic collision was also observed in a simulation carried out with the function $F$ corresponding to isotropic silica as substrate material (Fig. 7). With the comparatively large pulse widths chosen as initial conditions, radiation is no longer visible. From this finding one may conclude that the approximation of a constant function $F$ is not essential for having almost elastic collisions. Radiation can be enhanced by choosing narrow pulses having initial velocities close to each other.

The results of these numerical simulations suggest that the evolution equation (2.16) with KdV-type dispersion is, in some sense, close to an integrable system. We now demonstrate that this is indeed the case. With the approximation $F=\text{const}$ and with $\Delta(q)=\overline{\mu}_1 q$, Eq. (2.16) is readily converted into Eq. (3.11) for the Fourier transform of the surface elevation profile. With

$$U(\xi,\tau)=\int_0^\infty A(q,\tau)e^{iq\xi}\frac{dq}{2\pi}, \tag{5.2}$$

Eq. (3.11) is transformed into real space. It may be regarded as a special case of a one-parameter family of evolution equations,

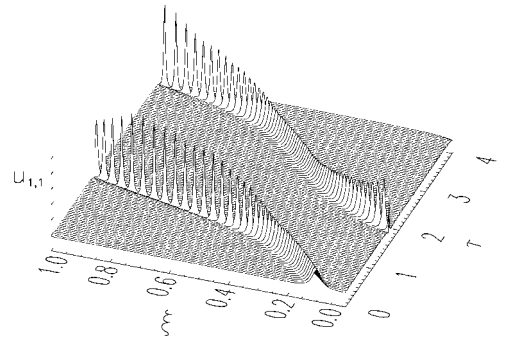


FIG. 8. Pulse evolution: BO-type linear dispersion, $F=\text{const}$. For the initial conditions see text.

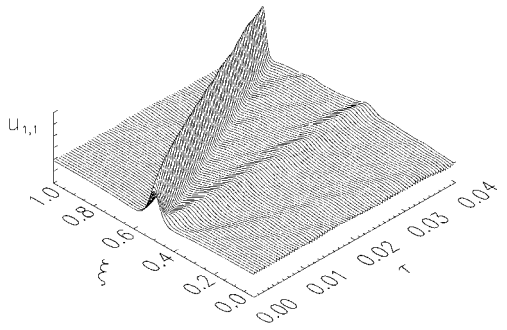


FIG. 9. Pulse evolution: KdV-type linear dispersion, $F=\text{const}$. For the initial conditions see text.

$$\frac{\partial}{\partial\tau}U=\frac{1}{4}(5\lambda-1)\frac{\partial^3}{\partial\xi^3}U+(\lambda-1)\hat{H}\left[\frac{\partial}{\partial\xi}U\right]\frac{\partial}{\partial\xi}U+\frac{\partial}{\partial\xi}\left\{\hat{H}\left[U\frac{\partial}{\partial\xi}U\right]+(2\lambda-1)U\hat{H}\left[\frac{\partial}{\partial\xi}U\right]-\frac{4}{9}\lambda U^3\right\}, \tag{5.3}$$

with the parameter $\lambda$ ranging from 0 to 1. ($\hat{H}$ denotes again the Hilbert transform.) In the limiting case $\lambda=0$, Eq. (5.3) is the real-space version of Eq. (3.11) (after rescaling)—i.e., the evolution equation for the surface elevation profile associated with nonlinear Rayleigh waves for a special choice of the acoustic mismatch between substrate and film and for an approximation of the nonlinearity that is well justified for fused quartz as substrate material. In the limit $\lambda=1$, Eq. (5.3) is the $BO_3$ equation—i.e., the third member of the Benjamin-Ono hierarchy analyzed by Case [54]. It has multisoliton solutions and hence elastic pulse collisions.

It is easily shown that Eq. (5.3) has the solitary wave solution

$$U(\xi,\tau)=\frac{-3\sqrt{12\overline{\kappa}}}{4\overline{\kappa}(\xi-\overline{\kappa}\tau+\xi_0)^2+3}, \tag{5.4}$$

with parameters $\overline{\kappa}>0$ and $\xi_0$, independent of the parameter $\lambda$. This is most conveniently done with the Fourier-space version of Eq. (5.3). Therefore, the (approximate) evolution equation (3.11) for nonlinear SAWs in a coated substrate with special acoustic mismatch between film and substrate may be continuously transformed into an equation that has

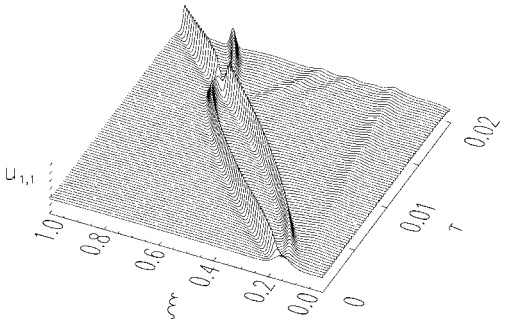


FIG. 10. Pulse evolution: KdV-type linear dispersion, $F=\text{const}$. For the initial conditions see text.

multisoliton solutions—namely, the $BO_3$ equation. This continuous transformation preserves the solitary wave solution. In this sense, Eq. (3.11) is "in the neighborhood of an integrable system," which may explain the numerical findings. However, we have to note that Eq. (5.3) contains an additional third-order nonlinearity for $\lambda \neq 0$. On the way from $\lambda = 0$ to $\lambda = 1$, the sign of the linear dispersion term changes at $\lambda = 1/5$. For this value of $\lambda$, one encounters the situation of a solitary wave existing even in the absence of linear dispersion. But this is not unusual as the combination of second-order and third-order nonlinearities in Eq. (5.3) is not scale invariant [55].

## VI. DYNAMICS WITH INITIAL CONDITIONS CLOSE TO A SOLITARY PULSE

The strong difference in the dynamical behavior described by Eq. (2.16) with BO-type dispersion on the one hand and KdV-type dispersion on the other is also reflected in the evolution of pulses that are initially close to a solitary solution. Figures 8–10 present the time evolution of pulses that correspond to solitary wave solutions enlarged by a factor $M$ at $\tau = 0$: $u^{(1)}_{\alpha,1}(x,0,0) = M\kappa S_\alpha(\kappa^{1/(\ell-1)}x)$. Figure 8 refers to BO-type dispersion, and the magnification factor has been chosen close to 1 ($M = 1.05$). Nevertheless, the deviation of the initial condition from that of a solitary pulse has a strong effect on the dynamics. The pulse is repeatedly accelerated and decelerated and, respectively, compressed and decompressed. This behavior is accompanied by the generation of radiation. Such a rolling picture in the $\xi - \tau$ plane is certainly not expected in integrable systems, where an infinite number of conservation laws strongly restricts the dynamics. The situation in Fig. 9, referring to KdV-type dispersion, is much more reminiscent of an integrable system. Here, the magnification factor $M$ has been chosen to be 2. From the initial condition, one large pulse and possibly several smaller pulses emerge and propagate with more or less constant speed. In addition, radiation is produced. However, when increasing the magnification factor to larger values ($M = 5$ in Fig. 10), a behavior is observed, even in the case of KdV-type dispersion, that is not expected to occur in integrable systems. From the initial conditions, two large solitary pulses emerge that initially propagate with different speed, then attract each other and perform a collision (i.e., overtake each other) with little radiation shed (Fig. 10). When following the two pulses further in time, one finds that the amount of radiation in the system increases and the two pulses do not seem to collide again.

In the simulations leading to the results exhibited in Figs. 8–10, the function $F$ in the evolution equation (2.16) was approximated by a constant. A systematic investigation of the pulse dynamics in this system with BO-type and KdV-type dispersions remains yet to be done. Such an investigation would have to examine in detail the influence of the finite spatial domain and periodic boundary conditions as they may especially affect the velocities of the pulses.

## VII. DEPTH PROFILE OF SOLITARY SOLUTIONS

The complicated depth structure of linear straight-crested SAWs, consisting of up to three partial waves, leads to non-

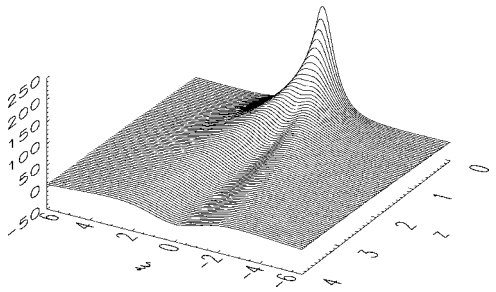

FIG. 11. Depth profile of solitary pulses. Substrate: fused silica, BO-type linear dispersion.

trivial depth profiles of solitary pulses and stationary periodic waves. With the traveling wave ansatz

$$\mathbf{u}^{(j)}(x,z,t) = \hat{\mathbf{u}}^{(j)}(x - v_R(1+\epsilon\kappa)t, z) \tag{7.1}$$

at each order $j$ in the asymptotic expansion (2.7), the depth profiles of solitary and periodic SAWs may be determined as expansions in powers of the parameter $\epsilon$—i.e., the typical strain. This has been discussed in some detail for the simpler system of nonlinear waves guided at the interface between a highly compressible fluid and a weakly compressible inhomogeneous solid, where the second-order contribution to the depth profile of a solitary pulse has been determined numerically [46]. From Eqs. (2.8), (2.9), and (3.1) and $B(q) = iqA(q)$, we obtain the leading-order term as

$$u^{(1)}_{\beta,1}(x,z,t) = \kappa\hat{S}_\beta(\kappa^{1/(\ell-1)}[x - v_R(1+\epsilon\kappa)t - x_0], \kappa^{1/(\ell-1)}z) \tag{7.2}$$

and

$$\hat{S}_\beta(x,z) = \int_0^\infty \frac{dq}{2\pi}\sum_{r=1}^{3} b_\beta(r)e^{q[ix+\alpha(r)z]}Q(q) + \text{c.c.}, \tag{7.3}$$

where $Q(q)$ is a solution of the nonlinear homogeneous integral equation (3.2). Figures 11 and 12 show examples of depth profiles $\hat{S}_1$ for fused silica as substrate and Si(111) $\langle 11\bar{2}\rangle$. In both cases, BO-type dispersion was assumed. If we approximate the function $F$ for the silica substrate by a constant and assume KdV-type dispersion, we obtain the following closed-form expression for $\hat{S}_1$:

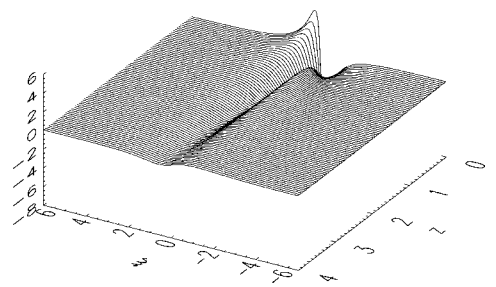

FIG. 12. Depth profile of solitary pulses. Propagation geometry: Si(111)$\langle 11\bar{2}\rangle$, BO-type linear dispersion.

$$\hat{S}_1(\xi,z)=\frac{\gamma}{\pi[1-\sqrt{\alpha(L)\alpha(T)}]}\left\{\frac{[\alpha(L)z-\beta]^2-x^2}{\{x^2+[\alpha(L)z-\beta]^2\}^2}-\sqrt{\alpha(L)\alpha(T)}\frac{[\alpha(T)z-\beta]^2-x^2}{\{x^2+[\alpha(T)z-\beta]^2\}^2}\right\}. \quad (7.4)$$

Here, $\alpha(L)=\sqrt{1-(v_R/v_L)^2}$, $\alpha(T)=\sqrt{1-(v_R/v_T)^2}$ and $v_L$ ($v_T$) are the velocities of longitudinal (transverse) bulk waves in the silica substrate. $\beta$ and $\gamma$ have been specified in Eqs. (3.12) and (3.13). The approximate analytic solution (7.4) gives an algebraic decay in the direction along the surface as well as in the direction normal to it. A plot of Eq. (7.4) looks very similar to Fig. 11.

Higher-order terms of the displacement gradients are determined by solving successively inhomogeneous linear boundary value problems. At each order, a compatibility condition has to be satisfied. The higher-order corrections determined in this way contain secular terms in the depth coordinate $z$. As mentioned already in Sec. II B, these terms have been criticized by Lardner [12] since they cause the solutions to be nonuniform. Lardner also pointed out that solutions uniformly valid up to depths of the order of $1/(\epsilon\overline{q})$, where $\overline{q}$ is a typical wave number, can be constructed by introducing a stretched depth coordinate and integrating the constraints (2.28). We show here how this construction works for stationary periodic solutions. In this case,

$$c_r(q,\eta,\tau)=2\pi\kappa\delta(q-nq_0)C_n^{(r)}(\kappa q_0\eta)e^{-inq_0\kappa\tau}/(inq_0). \quad (7.5)$$

In terms of the new amplitudes $C_n^{(r)}$ the constraint (2.28) takes the form

$$\frac{\partial}{\partial\eta}C_n^{(r)}(\eta)=-2ng(r)C_n^{(r)}(\eta)+nG(r)\sum_{m=1}^{n-1}C_m^{(r)}(\eta)C_{n-m}^{(r)}(\eta). \quad (7.6)$$

This has to be integrated with the initial conditions $C_n^{(r)}(0)=Q_n$ and $Q_n$ determined from Eq. (3.5). The result is

$$C_n(\eta)=\exp(-2ng\eta)\sum_{j=0}^{n-1}p_j^{(n)}\eta^j. \quad (7.7)$$

For the coefficients $p_j^{(n)}$, the following recursion relation is readily found:

$$p_j^{(n)}=\frac{n}{j}G\sum_{m=1}^{n-1}\sum_{\ell=1}^{m-1}p_\ell^{(m)}p_{j-\ell-1}^{(n-m)}\sigma(j-\ell-1|n-m-1) \quad (7.8)$$

for $j>0$ and $p_0^{(n)}=Q_n$. Here $\sigma(i|k)=1$ for $0\leqslant i\leqslant k$ and zero otherwise. This recursion relation can easily be implemented in numerical calculations. For simplicity, we have not explicitly indicated the dependence on $r$ in Eqs. (7.7) and (7.8).

## VIII. CONCLUSIONS

In the sections above, we have aimed at giving a comprehensive presentation of the theory of surface acoustic solitary waves and highlighting the agreement between calculations based on nonlinear elasticity theory and experimental results on solitary pulse shapes. The measurements were performed by pulsed laser excitation of high-intensity acoustic pulses in layered systems. As a main result, the anisotropy of the substrate was found to have a strong influence on the pulse shapes. It has been shown in numerical simulations that these solitary pulses normally perform highly inelastic collisions between each other. Only for a KdV-type linear dispersion law, which is realized by a special choice of linear acoustic mismatch between the substrate and a coating film, are SAW pulse collisions nearly elastic. An explanation for this finding is suggested which is based on the fact that in this special case, the evolution equation for nonlinear SAWs can be related to an equation of the Benjamin-Ono hierarchy.

An important feature of surface acoustic solitary waves is their two-dimensional character. They have a nontrivial depth profile which may be constructed from their associated strain distribution at the surface. The latter can be determined from a one-dimensional evolution equation with a strongly nonlocal second-order nonlinearity. The derivation of the evolution equation, as well as the reconstruction of the depth profile, was done with the help of asymptotic methods that have an approximate character and are valid for weak nonlinearity and weak dispersion. Different variants of the theory provided in the literature were compared, and it has been shown explicitly that three of them lead to the same evolution equation. With these asymptotic methods stationary periodic solutions of the equations of nonlinear elasticity were constructed that are uniformly valid up to depths of the order of a typical wavelength divided by a typical strain.

Due to the absence of material dispersion in the acoustics of solids, there are several physical systems where acoustic waves are nondispersive. By modification of the propagation geometry, dispersion can be introduced and tailored in a controlled way. One example is the system investigated here—namely (generalized), Rayleigh waves propagating along the planar surface of a homogeneous elastic half-space. Normal and anomalous dispersion of the SAWs was realized by depositing a thin isotropic film onto the substrate. Other types of guided acoustic waves that are ideally nondispersive include Bleustein-Gulyaev waves, wedge acoustic waves, Stonely waves, etc. Nonlinear effects in these nondispersive systems have partly been studied already, and evolution equations with nonlocal nonlinearity have been derived [56–58,33]. When dispersion is introduced into these systems, solitary waves are expected to exist. The nonlinearity in the corresponding evolution equations is partly of third order. Effective evolution equations with nonlocal nonlinearity of third order have also been derived in the field of nonlinear optics for pulse propagation in dispersion-managed fibers [59,60], and solitary solutions for such equations have been determined numerically [61]. An important difference is the scale invariance of the nonlinearity of homogeneous elastic media in the acoustics context, which poses a challenge for future investigations.

[1] A more general definition includes stationary excitations that are spatially localized by nonlinearity.
[2] A. Scott, *Nonlinear Science—Emergence and Dynamics of Coherent Structures* (Oxford University Press, Oxford, 1999).
[3] A. M. Samsonov, *Strain Solitions in Solids and How to Construct Them* (Chapman & Hall/CRC, Boca Raton, 2001).
[4] H.-Y. Hao and H. J. Maris, Phys. Rev. B **64**, 064302 (2001).
[5] A. M. Lomonosov and P. Hess, Phys. Rev. Lett. **83**, 3876 (1999).
[6] A. M. Lomonosov, P. Hess, and A. P. Mayer, Phys. Rev. Lett. **88**, 076104 (2002).
[7] M. J. Ablowitz and P. A. Clarkson, *Solitons, Nonlinear Evolution Equations and Inverse Scattering* (Cambridge University Press, Cambridge, England, 1991).
[8] D. F. Parker, in *Nonlinear Waves in Solid State Physics*, edited by A.D. Boardman, T. Twardowski, and M. Bertolotti (Plenum, New York, 1990), p. 163.
[9] J. K. Hunter, Contemp. Math. **100**, 185 (1989).
[10] M. F. Hamilton, Yu. A. Il'insky, and E. A. Zabolotskaya, J. Acoust. Soc. Am. **97**, 882 (1995).
[11] D. F. Parker and J. K. Hunter, Supplemento ai Rendiconti del Circolo Matematico di Palermo, Serie II, No. 57 (1998).
[12] R. W. Lardner, Int. J. Eng. Sci. **21**, 1331 (1983); J. Appl. Phys. **55**, 3251 (1984); J. Elast. **16**, 63 (1986).
[13] D. F. Parker and F. M. Talbot, J. Elast. **15**, 389 (1985).
[14] D. F. Parker, Phys. Earth Planet. Inter. **50**, 16 (1988).
[15] D. F. Parker, Int. J. Eng. Sci. **26**, 59 (1988).
[16] E. A. Zabolotskaya, J. Acoust. Soc. Am. **91**, 2569 (1992).
[17] E. Yu. Knight, M. F. Hamilton, Yu. A. Il'insky, and E. A. Zabolotskaya, J. Acoust. Soc. Am. **102**, 1402 (1997).
[18] M. F. Hamilton, Y. A. Il'inskii, and E. A. Zabolotskaya, J. Acoust. Soc. Am. **105**, 639 (1999).
[19] G. Leibfried and W. Ludwig, Z. Phys. **160**, 80 (1960).
[20] H. F. Tiersten, J. Appl. Phys. **40**, 770 (1969).
[21] A. A. Maradudin, in *Physics of Phonons*, edited by T. Paszkiewicz (Springer, New York, 1987), p. 82.
[22] A. S. Kovalev, A. P. Mayer, C. Eckl, and G. A. Maugin, Phys. Rev. E **66**, 036615 (2002).
[23] V. P. Reutov, Izv. Vyssh. Uchebn. Zaved., Radiofiz. **16**, 1690 (1973) [Radiophys. Quantum Electron. **16**, 1307 (1973)].
[24] A. P. Mayer and A. A. Maradudin, in *Continuum Models and Discrete Systems*, edited by G. A. Maugin (Longman, London, 1991), Vol. 2, p. 306.
[25] D. F. Parker, A. P. Mayer, and A. A. Maradudin, Wave Motion **16**, 151 (1992).
[26] A. P. Mayer, Phys. Rep. **256**, 237 (1995).
[27] A. M. Lomonosov, A. P. Mayer, and P. Hess, in *Modern Acoustical Techniques for the Measurement of Mechanical Properties*, edited by M. Levy, H. E. Bass, and R. Stern, Experimental Methods in the Physical Sciences, Vol. 3 (Academic, San Diego, 2001), p. 65.
[28] E. H. Bogardus, J. Appl. Phys. **36**, 2504 (1965).
[29] W. T. Yost and M. A. Breazeale, J. Appl. Phys. **44**, 1909 (1973).
[30] J. J. Hall, Phys. Rev. **161**, 756 (1967).
[31] D. F. Parker and E. A. David, Int. J. Eng. Sci. **27**, 565 (1989).
[32] A. V. Porubov and A. M. Samsonov, Int. J. Non-Linear Mech. **30**, 861 (1995).
[33] G. D. Meegan, M. F. Hamilton, Yu. A. Il'inskii, and E. A. Zabolotskaya, J. Acoust. Soc. Am. **106**, 1712 (1999).
[34] The existence of a Lagrangian in the nondispersive case has been known a long time, and the Hamiltonian structure associated with Eq. (2.16) was derived by P. Panayotaros, Phys. Lett. A **289**, 111 (2001).
[35] V. I. Nayanov, Pis'ma Zh. Eksp. Teor. Fiz. **44**, 245 (1986) [JETP Lett. **44**, 314 (1986)].
[36] Y. Cho and N. Miyagawa, Appl. Phys. Lett. **63**, 1188 (1993).
[37] V. Kavalerov, H. Katoh, N. Kasaya, M. Inoue, and T. Fujii, Jpn. J. Appl. Phys., Part 1 **34**, 2653 (1995).
[38] J. F. Ewen, R. L. Gunshor, and V. H. Weston, J. Appl. Phys. **53**, 5682 (1982).
[39] V. E. Gusev, W. Lauriks, and J. Thoen, Phys. Rev. B **55**, 9344 (1997).
[40] V. E. Gusev, W. Lauriks, and J. Thoen,, J. Acoust. Soc. Am. **103**, 3203 (1998).
[41] Al. A. Kolomenski, A. M. Lomonosov, R. Kuschnereit, P. Hess, and V. E. Gusev, Phys. Rev. Lett. **79**, 1325 (1997).
[42] A. A. Kolomenski and H. A. Schuessler, Phys. Lett. A **280**, 157 (2001).
[43] Al. A. Kolomenski and H. A. Schuessler, Phys. Rev. B **63**, 085413 (2001).
[44] M. F. Hamilton, Yu. A. Il'insky, and E. A. Zabolotskaya, J. Acoust. Soc. Am. **97**, 891 (1995).
[45] G. Ali and J. K. Hunter (unpublished).
[46] A. P. Mayer and A. S. Kovalev, Proc. Est. Acad. Sci., Phys., Math. **52**, 43 (2003).
[47] A. Norris, in *Proceedings of the 1992 IEEE Ultrasonics Symposium*, edited by B. R. McAvoy (IEEE, New York, 1992), p. 671, and references therein.
[48] H. Ono, J. Phys. Soc. Jpn. **39**, 1082 (1975).
[49] J. A. Scales and A. E. Malcolm, Phys. Rev. E **67**, 046618 (2003).
[50] A. M. Lomonosov and P. Hess, Phys. Rev. Lett. **89**, 095501 (2002).
[51] W. H. Press, S. A. Teukolsky, W. T. Vetterling, and B. P. Flannery, *Numerical Recipes in Fortran*, 2nd ed. (Cambridge University Press, Cambridge, England, 1992).
[52] C. Eckl, A. P. Mayer, and A. S. Kovalev, Phys. Rev. Lett. **81**, 983 (1998).
[53] C. Eckl, J. Schöllmann, A. P. Mayer, A. S. Kovalev, and G. A. Maugin, Wave Motion **34**, 35 (2001).
[54] K. M. Case, Physica D **3**, 185 (1981).
[55] Hunter has given an example of an evolution equation with scale-invariant second-order nonlinearity and no linear dispersion that admits solitary solutions (Ref. [9]). Here, the nonlinearity is of a form that precludes generation of higher harmonics from a sinusoidal wave.
[56] A. P. Mayer, Int. J. Eng. Sci. **29**, 999 (1991).
[57] V. V. Krylov and D. F. Parker, Wave Motion **15**, 185 (1992).
[58] A. P. Mayer, V. G. Mozhaev, V. V. Krylov, and D. F. Parker, in *Nonlinear Coherent Structures in Physics and Biology*, edited by K. H. Spatschek and F. G. Mertens (Plenum, New York, 1994), p. 279.
[59] M. J. Ablowitz and G. Biondini, Opt. Lett. **23**, 1668 (1998).
[60] S. K. Turitsyn, T. Schäfer, K. H. Spatschek, and V. K. Mezentsev, Opt. Commun. **163**, 122 (1999).
[61] M. J. Ablowitz, G. Biondini, and E. S. Olson, J. Opt. Soc. Am. B **18**, 577 (2001).
[62] V. Gusev, C. Glorieux, and J. Thoen, J. Acoust. Soc. Am. **103**, 2946 (1998).